

Outburst activity in comets – II. A multiband photometric monitoring of comet 29P/Schwassmann–Wachmann 1

Josep M. Trigo-Rodríguez,^{1,2*} D. A. García-Hernández,^{3,4} Albert Sánchez,⁵ Juan Lacruz,⁶ Björn J. R. Davidsson,⁷ Diego Rodríguez,⁸ Sensi Pastor⁹ and José A. de los Reyes⁹

¹*Institute of Space Sciences (CSIC), Campus UAB, Facultat de Ciències, Torre C-5 pares, 2a pl., 08193 Bellaterra (Barcelona), Spain*

²*Institut d'Estudis Espacials de Catalunya (IEEC), Ed. Nexus, Gran Capità 2-4, 08034 Barcelona, Spain*

³*Instituto de Astrofísica de Canarias (IAC), E-38200 La Laguna, Tenerife, Spain*

⁴*Universidad de La Laguna (ULL), E-38205 La Laguna, Tenerife, Spain*

⁵*Gualba Astronomical Observatory (MPC442), Barcelona, Spain*

⁶*La Cañada Observatory (MPC J87), Ávila, Spain*

⁷*Department of Physics and Astronomy, Uppsala University, Box 516, SE-75120, Uppsala, Sweden*

⁸*Guadarrama Observatory (MPC458), Madrid, Spain*

⁹*Observatorio Astronómico Municipal de Murcia (J76), La Murta, Murcia, Spain*

Accepted 2010 July 23. Received 2010 July 19; in original form 2010 April 21

ABSTRACT

We have carried out a continuous multiband photometric monitoring of the nuclear activity of comet 29P/Schwassmann–Wachmann 1 from 2008 to 2010. Our main aim has been to study the outburst mechanism on the basis of a follow-up of the photometric variations associated with the release of dust. We have used a standardized method to obtain the 10-arcsec nucleus photometry in the *V*, *R* and *I* filters of the Johnson–Kron–Cousins system, which are accurately calibrated with standard Landolt stars. The production of dust in the *R* and *I* bands during the 2010 February 3 outburst has been also computed. We conclude that the massive ejection of large (optically thin) particles from the surface at the time of the outburst is the triggering mechanism to produce the outburst. The ulterior sublimation of these ice-rich dust particles during the following days induces fragmentation, generating micrometre-sized grains, which increase the dust spatial density to produce the outburst in the optical range as a result of the scattering of sunlight. The material leaving the nucleus adopts a fan-like dust feature, formed by micrometre-sized particles that decay in brightness as it evolves outwards. By analysing the photometric signal measured in a standardized 10-arcsec aperture using the phase dispersion minimization technique, we have found a clear periodicity of 50 d. Remarkably, this value is also consistent with an outburst frequency of 7.4 outbursts per yr deduced from the number of outbursts noticed during the effective observing time.

Key words: comets: individual: 29P/Schwassmann–Wachmann 1.

1 INTRODUCTION

For a long time, comet 29P/Schwassmann–Wachmann 1 (hereafter SW1) has been considered the archetype of comets exhibiting unusual changes in their coma appearance and brightness (Sekanina 1982). SW1 moves along a quasi-circular orbit with eccentricity $e \sim 0.044$ and semimajor axis $a \sim 6$ au (Marsden & Williams 2003). A key goal of photometric monitoring is to deduce the comet rotation period from the observed activity. This idea is not new; the

first attempts to do so with comet 29P were performed many years ago (see, for example, Whipple 1980; Meech et al. 1993; Cabot et al. 1997). In any case, many difficulties arise in trying to understand the outbursts of 29P and its photometric behaviour. During an outburst, the nuclear magnitude typically increases by 2 or 5 mag in a behaviour that seems unusual, but which would be typical for primitive objects such as, for example, centaurs and trans-Neptunian objects (TNOs) located at the appropriated heliocentric distances. As we have pointed out previously, being so far away from the Sun, its surface temperature is below the sublimation of water ice so other physical processes are suspected of playing a role in generating outbursts (Trigo-Rodríguez et al. 2008, hereafter Paper I). In

*E-mail: trigo@ieec.uab.es

Table 1. Observatories, telescopes, resolutions and people involved.

Observatory	MPC code	Telescope	Resolution (arcsec)	Longitude (°)	Latitude (°)	Observer
Gualba, Barcelona	442	SC 36.0 <i>f</i> /7	1.6	2° 31′ 15″ E	41° 43′ 16″ N	A. Sánchez
Guadarrama, Madrid	458	SC 25 <i>f</i> /6.3	2.3	4° 01′ 20″ W	40° 38′ 14″ N	D. Rodríguez
IAC-80, Teide, Tenerife	954	C 82 <i>f</i> /11.3 par	0.5	16° 30′ 33.4″ E	28° 17′ 53.6″ N	D. A. García-Hernández et al.
La Cañada Observatory	J87	RC 40 <i>f</i> /10	1.2	4° 29′ 30″ W	40° 36′ 18″ N	J. Lacruz
Montseny Obs., Girona	B06	N 18 <i>f</i> /6	1.5	2° 31′ 14″ E	41° 43′ 17″ N	J. M. Trigo-Rodríguez

Paper I, we presented a detailed 5-yr photometric monitoring. Despite the fact that previously such follow-ups were mainly performed by relatively small telescopes, interesting conclusions on the activity of this centaur were obtained. However, other important issues about the mechanism producing these outbursts and the periodicity of this activity have remained open to question. Since the publication of Paper I, we have continued our monitoring of this object with three main objectives: (i) to take a step forward in monitoring this object by using multiband photometry in different Johnson–Kron–Cousin standard filters; (ii) to use Landolt and Stetson calibration fields to accurately calibrate the photometric estimations in order to find the accuracy of 10-arcsec nuclear photometry in the different filters; (iii) to identify the periodicity and plausible triggering mechanism producing these outbursts.

The results of Paper I encouraged us to continue our follow-up of SW1 activity to learn more about the processes that take place in the coma after an outburst. Because of the energy driven by the explosive activity on the surface of 29P, we previously suggested that mm-sized particles leave the surface and that their progressive sublimation in the coma causes the peculiar coma evolution behaviour described in Paper I. Our multiband monitoring confirms such an explanation, being consistent with the reflectivity variations observed in the coma of this comet after the outbursts. In Section 2, we have compiled the observational data and reduction procedures taken into account in this work. In Section 3, we describe the outbursts detected during the 2008–2010 observational period, some of which have been widely monitored in different photometric bands. In Section 4, we discuss the implications of our observations for explaining cometary activity and the dust processes taking place in the coma. Our final conclusions are summarized in Section 5.

2 OBSERVATIONAL DATA AND REDUCTION PROCEDURE

We have performed multiband CCD photometry from several amateur and professional observatories (Table 1). Table 1 shows a log of the observatories used together with some relevant information such as telescope, instrument, resolution and observers. Optical photometry in the Johnson *V*, *R* and *I* filters was obtained with the IAC-80 telescope (Observatorio del Teide, Spain) equipped with the CAMELOT CCD (see, for example, <http://www.iac.es/telescopes/iac80/CCD.htm> for more details). The IAC-80 Johnson *VRI* magnitudes were derived using standard aperture photometry tasks in the IRAF software.¹ The data reduction process basically consists of bias subtraction, flat-field correction and flux calibration. This time, the nuclear photometric accuracy given for a stan-

dard aperture of 10 arcsec has been improved compared to Paper I by using Landolt and Stetson calibration fields (Landolt 1992; Stetson 2000). The photometric reduction procedure for small-sized telescopes was performed by using an additional software package called LAIA (after the Laboratory for Astronomical Image Analysis), successfully tested for obtaining high-precision stellar photometry (García-Melendo & Clement 1997; Escolà-Sirisi et al. 2005). The procedure is similar to that described by Snodgrass, Lowry & Fitzsimmons (2006), but limited to our 10-arcsec selected aperture. Using these standards, we were able to quantify the typical data accuracy to be better than 0.05 mag in the different *VRI* bands. These results clearly improve the 0.1–0.2 error in *R* magnitude obtained in Paper I. The spatial scale obtained by our instruments is between 0.3 and 2.3 arcsec pixel⁻¹, which corresponds to resolutions of about 1255 and 9625 km pixel⁻¹, respectively, at the Earth–comet distance $\Delta = 5.77$ au (see Table 1 for more details). These ideal values are typically affected by seeing, so the effective resolution is between 1 and 2 arcsec, or roughly about 6300 km pixel⁻¹. Our experience says that such a resolution is good to follow the overall nuclear activity of this centaur using the above-mentioned standard aperture (Trigo-Rodríguez et al. 2008).

A total of 498 photometric measurements of SW1 in the different filters have been considered in this paper, although our monitoring is still continuing. The data were obtained by eight experienced observers on 217 nights between 2008 January and 2010 June. This monitoring can be considered complementary to the 5-yr follow-up presented by our team in Paper I. The observational data obtained by our team are available to other cometary scientists on request.

3 OBSERVATIONAL RESULTS

The complete set of photometric observations obtained in this work is shown in Fig. 1. The data profile show evidence of good coverage except for the periods when the comet was in conjunction with the Sun. In the following, we describe some of the most important features that were detected in our monitoring of the outbursts.

Following the criterion described in Paper I, where we counted as an outburst any increase in 1 mag in the coma brightness, we can identify the main bursts in the photometric profile. Taking this criterion into account, our data reveal 11 outbursts from 2008 January to 2010 February (see Fig. 1). Because of the weather conditions, some of these are better covered than others. The different outbursts detected and several parameters to describe their particular strength are included in Table 2. Note that this table shows not only the increase in magnitude, but also the amplitude interval among consecutive outbursts. We have found that a significant number of outbursts occur after 20–40 d.

In Fig. 1 we can see evidence of two main types of outbursts, which we call single and multiple. Single outbursts exhibit a progressive increase and decrease in the coma magnitude. Good examples of a single outburst are those labelled in Table 1 as A, C,

¹ IRAF is distributed by the National Optical Astronomy Observatories, which is operated by the Association of Universities for Research in Astronomy, Inc., under cooperative agreement with the National Science Foundation.

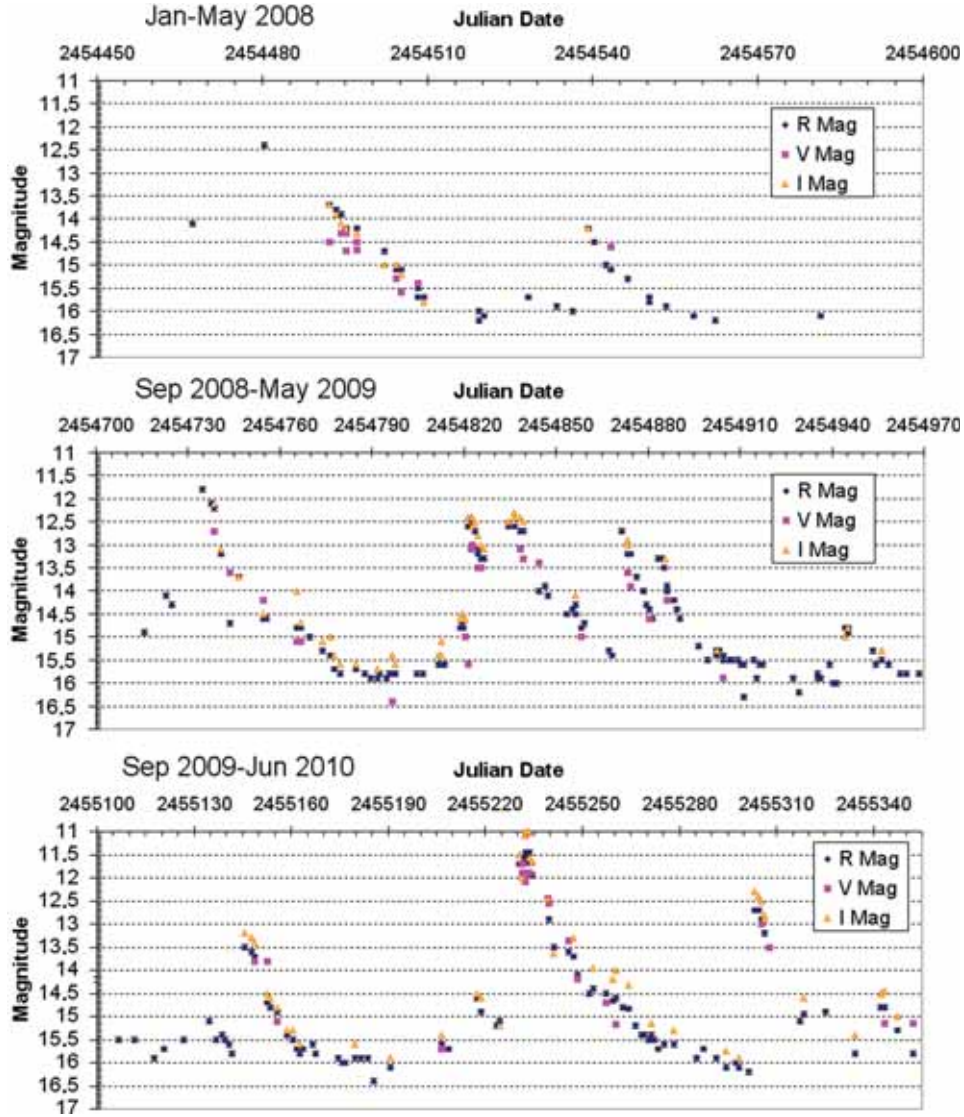


Figure 1. Photometric coverage using the different Johnson–Kron–Cousins filters during the monitored period. Error bars are not shown at the present image resolution, but magnitude accuracy was found to be better than 0.05 mag.

Table 2. Specific details of the detected outbursts. The peak amplitude denotes the approximate time required for the comet to reach the maximum brightness (up) or to return (down) to a quiescent stage. This value is only given for those cases in which the outburst is well covered. Tentative values in the case of poor coverage are given in parentheses.

Outburst date	Julian date	Peak label	Observed peak <i>R</i> magnitude (mag)	Magnitude increase (mag)	Peak semi-amplitude (d) Up	Down
2008 Jan 14.8	245 4480.4	A	+12.4	3.8	–	39
2008 Mar 13.8	245 4539.3	B	+14.2	2.0	–	23
2008 Sep 25.1	245 4734.6	C	+11.8	4.1	–	57
2008 Dec 23.2	245 4822.7	D	+12.5	3.3	16	–
2009 Jan 3.1	245 4834.5	E	+12.6	1.0	–	24
2009 Feb 8.8	245 4871.4	F	+12.7	2.7	13	10
2009 Feb 21.7	245 4884.3	G	+13.3	1.3	4	31
2009 Apr 22.8	245 4944.3	H	+14.8	1.4	30	(23)
2009 Sep 23.1	(245 5097.6)	I	(+13.9)	(2.0)	–	20
2009 Nov 10.2	245 5145.6	J	+13.5	2.4	28	40
2010 Feb 3.2	245 5230.7	K	+11.7	4.3	46	–
2010 Apr 16.8	245 5303.3	L	+12.7	3.5	30	(19)

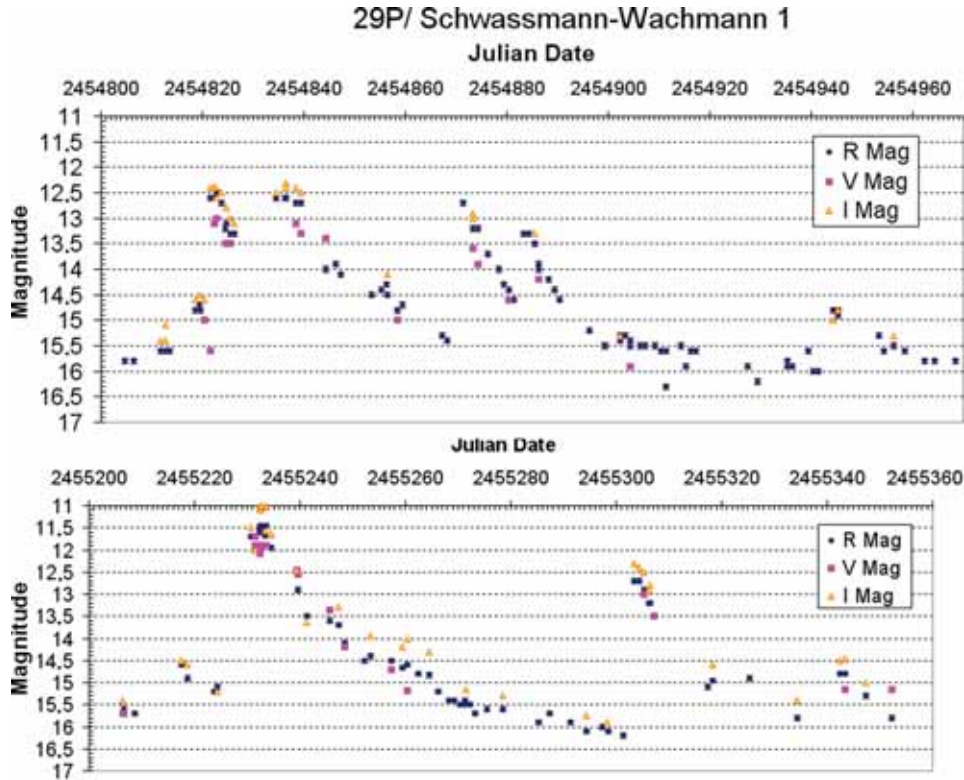


Figure 2. Detailed plots of the photometric profile showing the best sampled outbursts plotted in Fig. 1. (a) Photometric curve in the different filters showing the double-peak behaviour exhibited from 2008 December to 2009 May. (b) Detailed photometry around the 2010 February 2 outburst, showing the observations made during the first semester of 2010. Note that the error bars (0.05 mag) are not visible at this scale.

H, J, K and L. In these cases, the activity increases progressively in about 20 or 30 d. The multiple outburst behaviour is exemplified by the sequence of outbursts listed from D to G. There is a very simple explanation behind this behaviour: the presence of multiple active regions, which, as the nucleus rotates, are exposed periodically to solar radiation. More details are presented in the discussion, but note that a nucleus with several active regions rotating every 50 d can explain the photometric behaviour.

The period between JD 245 4800 and 245 4960 is shown in a separate window in Fig. 2(a). We remark that the activity profile starts to grow progressively from a quiescent period at magnitude +15.8 R until reaching a peak called D at +12.5 R on JD 245 4822.7. All the upwards profile is characterized by high I magnitude values. Only 12 d after this, just on JD 245 4834.6, we can see peak E with a similar strength. Note that the pattern of two peaks reappears on JD 245 4871.4 and JD 245 4883.4 (peaks F and G) with a similar spacing of 12 d (but in this case much better sampled). Note that both peaks are repeated after 50 d. Curiously, despite the good data sampling, this pattern disappears because the following outburst occurs on JD 245 4944.3.

Our best monitored outburst took place around 2010 February 2, and has been included in full detail in Fig. 2(b). We posted an alert to the astronomical community about this unusually bright outburst (Trigo-Rodríguez et al. 2010). On February 3.18 the first multiband photometry was obtained from the Gualba Observatory (MPC442), which shows the comet exhibiting a bright core characteristic of a massive outburst (Fig. 3). At this time, the photometry of the 10-arcsec standard aperture shows an infrared increase that makes the nuclear magnitude brighter in I than in the R or V bands. The bright dust globule formed by the release of dust particles evolves

outwards, as confirmed by high-resolution additional observations taken from IAC-80 (Fig. 4).

4 DISCUSSION

4.1 Periodicity of 29P outbursts

To better understand the physical processes behind the production of outbursts by 29P, its rotation period is a key parameter that needs to be constrained. Different researchers have been trying this, but there are large discrepancies in the literature. We think that the most probable origins for these discrepancies are insufficient or biased data sampling. To cite some examples of published period data in order of decreasing value, Stansberry et al. (2004) reported a rotation period of about 60 d or more, while Trigo-Rodríguez et al. (2008) and Moreno (2009) found a rotation period of about 50 d, emphasizing the need for more precise observational data. Finally, shorter periods of 6 and 4.97 d were found by Jewitt (1990) and Whipple (1980), respectively. Meech et al. (1993) suggested that the nucleus exhibits a complex spin state with two very short periods of 14 and 32 h. Obviously, the characterization of the spin rate of the 29P nucleus from observational data requires good coverage and also very accurate observational data. In this regard, the more accurate photometric accuracy (at least 0.05 mag) of the 2008–2010 data presented here, in comparison with our previous coverage presented in Paper I, allows us to better study the existence of periodicity in the photometric profile. Because the data sampling is unevenly spaced, we have used different tools in the periodogram analysis, including the precise determination of minimums by the same software *AVE* that we used previously (Trigo-Rodríguez et al.

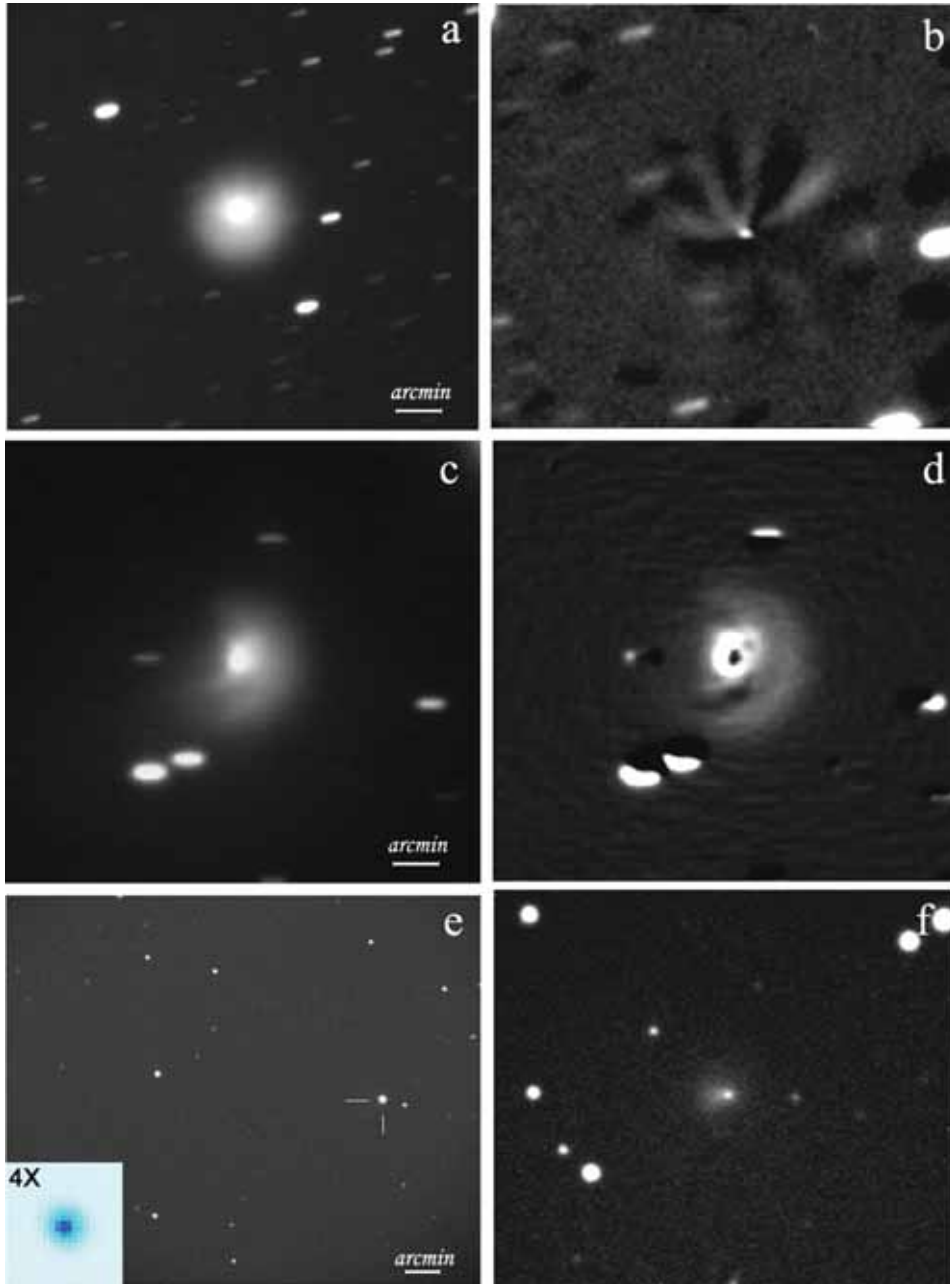


Figure 3. Some images exemplifying the changing appearance of comet 29P. (a) A 42-min stack image obtained about two weeks after outburst C (see Table 2 for further details). Taken from the MPC J87 observatory by J. Lacruz on JD 245 4743.6. (b) Larson–Sekanina filtered image of (a), rotated by 15° , showing the multiple jets that formed the fan in the previous image. (c) A 45-min stack image taken from J87 on JD 245 4877.4, just one week after outburst F. (d) Larson–Sekanina filtered image of (c), rotated by 15° , and shifted by 0.5 pixels to better see the fan structure. (e) Stellar appearance of 29P just after the outburst K, when the comet was in $+11.7 R$ magnitude. A 3-min stack image taken from MPC 442 by A. Sánchez on JD 245 5231.5. (f) Pre-outburst image of (e), taken with the same instrument from MPC 442 on JD 245 5223.7 when the comet was in $+15.2 R$ magnitude. Note that the scale of the images on the right-hand side is identical to those shown on the left.

2008). Basically, we used the phase dispersion minimization (PDM; Stellingwerf 1978) and the discrete Fourier transform (Deeming 1975) methods. As the results of both methods are similar, for simplicity here we discuss only PDM periodograms.

The PDM periodograms are shown in Fig. 5. For the purpose of discussing the values given in the literature, we have separated the periodogram into two plots, one for short periods of less than 10 d (Fig. 5a) and the other for periods up to 100 d. We note that there is no evidence of periodicity in the signal in Fig. 5(a), except for the

period of 1 d, which is an alias produced by the typical 24-h observational window. This periodogram is so clean that it demonstrates that the comet’s activity during 2008–2010 was not hiding a periodicity lower than 10 d. In other words, if the profile activity is a reflex of the active regions in the nucleus, its rotation was not in the plotted periodicity window. Fortunately, the second periodogram shown in Fig. 5(b) includes additional clues with three clear peaks over the noise. The most obvious is 66.94 ± 0.03 d, followed by another at 55.21 ± 0.07 d, and a third at 50.02 ± 0.07 d. The first value of about

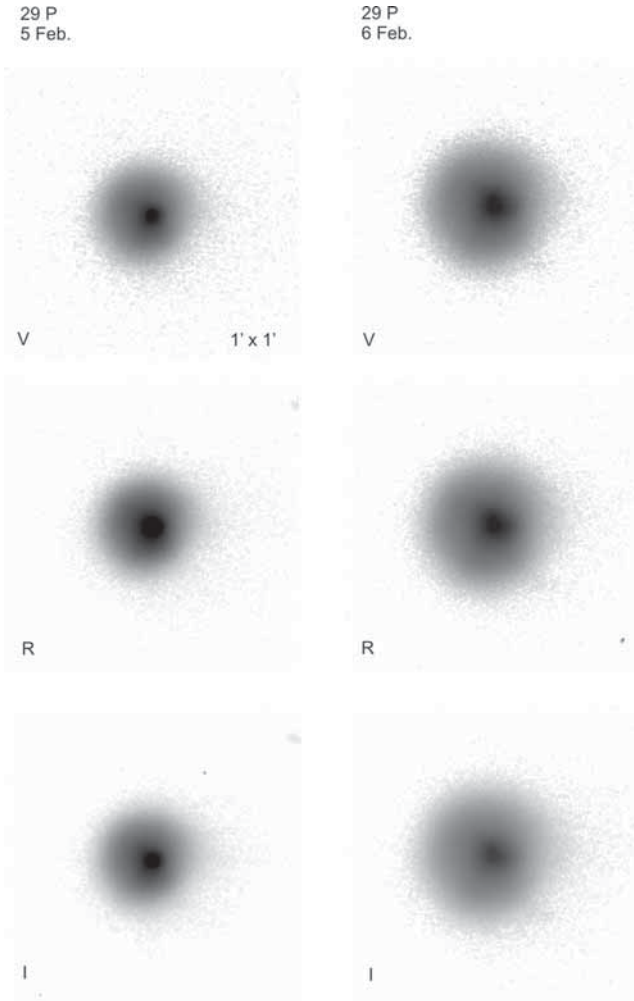


Figure 4. The expanding coma after the outburst, as imaged with the IAC-80 telescope with the different *VRI* filters for February 5.09 (left images) and February 6.08 (right images). The images are shown using a logarithmic scale.

67 d is just an alias (i.e. period combination) for the synodic period of about 392 d, as we also found in Paper I. This idea is reinforced by the fact that an additional exploration of larger periodicities has also shown synodic period aliases for 128 and 200 d. Consequently, we think that the 50-d period can be given as a tentative value for the rotation period of this comet. In any case, we should be cautious when identifying the outburst period with the rotational period. The two may be related, but the former could be a low-number multiple of the latter because the number of rotational periods between outbursts could also vary stochastically, as apparently is also the case for 9P/Tempel 1 (Belton et al. 2008). Moreover, such a large period seems to be unusual among the population of TNOs and centaurs, which exhibit rotation periods typically lower than 1 d (Sheppard, Lacerda & Ortiz 2008), and also for other comets (Samarasinha et al. 2004). Note also that we have not constructed and compared our observational results with the theoretical rotationally phased light curve, as this is difficult to do for this object. It is obvious that the intensity of the outbursts is highly variable and also depends on the reliability of the observational coverage. Despite this, taking into account the two periods where the comet was in solar conjunction (about 263 d without observations in our sample), the average outburst frequency during the effective observing period

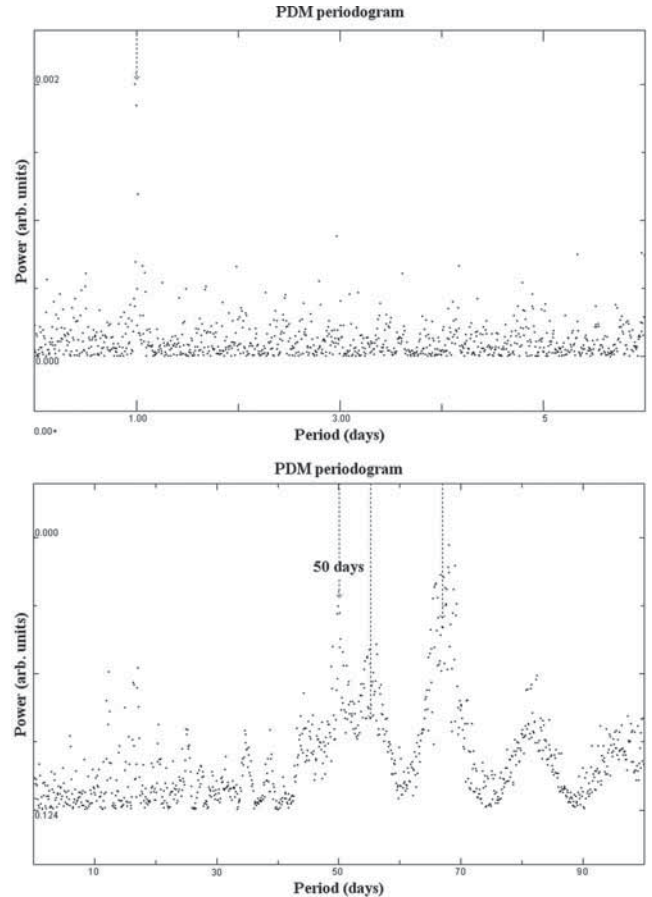


Figure 5. Periods shown by PDM periodograms. The peak for a nucleus periodicity $P = 50.02 \pm 0.07$ d is shown. For more details on the other peaks, see the text.

was 49 d. Note that this value is again consistent with the deduced rotation period from periodograms. Such a frequency corresponds to 7.4 outbursts per yr, which is almost identical to the value previously found by our team (Trigo-Rodríguez et al. 2008). Note that this periodicity might be directly related to the rotational period of this comet, but we cannot rule out that it is just a multiple of such a period. The spurious (less defined) secondary peak at about 55 d would be a consequence of additional active areas exhibiting sporadic activity, or other irregularities caused by the stochastic evolution of the surface or subsurface properties.

4.2 Quantifying the dust production: $Af\rho$

In the previous sections, we have shown that our observations suggest that several active areas are producing dust on the surface of this centaur. The scenario seems to be complex, and highly variable as a function of time. For example, the observed activity pattern between 2008 December and 2009 May (plotted in Fig. 2a) can be explained by the presence of two regions becoming active every 50 d. Although the data sampling is not complete after peak G, it seems that the double-peak pattern disappears after this. Were the active regions collapsing (under rubble) or was the activity damped for another reason? From the important variations in the active regions with time, it seems that the different strengths of each outburst could be a consequence of resurfacing (e.g. some released materials are participating in covering the active regions). In a similar way, the creation of new active areas can also be explained in the context

of tensile strength variations on the surface as consequence of the crystallization of amorphous ice (Priainik 2000; Trigo-Rodríguez & Blum 2009). Consequently, a long time surface processing as that described above might explain some of the features observed in several comets, particularly the layering observed in comet 9P/Tempel 1 studied by Deep Impact spacecraft (Belton et al. 2007). However, without clear data on the rotational axis, we think that it is not possible to discard other possibilities associated with a changing-tilt geometry. For example, if the rotation axis was complex, some regions would be exposed to sunlight from time to time. Perhaps this is not so likely, taking into account the 50-d periodicity behind most of the outbursts.

We suggested in Paper I that the source of the energy driving cometary outbursts could be associated with the explosive sublimation of ice-rich regions, which, after a massive breakup of the surface, are exposed to solar radiation (Trigo-Rodríguez et al. 2008). This massive release of material is produced from active regions of the surface. The larger the region, the more massive the release of material participating in the outburst. The variability could then be explained by the formation of a rubble mantle (see, for example, Jewitt 2008), perhaps because of the collapse of the region when volatile depletion reduces the tensile strength of the surface. Another possibility is the accumulation of large particles that cannot escape the nucleus. Stansberry et al. (2004) used thermal models fitted to photometry at 8, 24 and 70 μm for *Spitzer* observations to estimate a nuclear radius of 27 ± 5 km. The escape velocity (V_{esc}) is defined as the minimum velocity that a grain needs to win the gravitatory attraction of the nucleus. This is calculated from the well-known equation:

$$V_{\text{esc}} = \sqrt{\frac{2GM_c}{R_c}}. \quad (1)$$

By considering a comet radius of 27 km, and assuming a spherical shape for the nucleus with a bulk density of 1000 kg m^{-3} , we have derived $V_{\text{esc}} \approx 20 \text{ m s}^{-1}$. In Paper I we found that a 1 mm diameter meteoroid with an assumed bulk density of 500 kg m^{-3} typically leaves the nucleus at $V_{\text{ej}} \approx 22 \text{ m s}^{-1}$. We note that $V_{\text{ej}} \propto \text{m}^{-1/6}$ and, consequently, the impulse for large meteoroids decreases significantly. For example, a 1 cm diameter particle with the same density would have $V_{\text{ej}} \approx 7 \text{ m s}^{-1}$, which is clearly inferior to the escape velocity for this comet. Consequently, the nucleus gravity creates a cut-off for large particles. However, we should note that the 5–100 μm particles escaping the SW1 nucleus are virtually unobservable in cometary comae at visual wavelengths. However, we want to note that the previous simplistic approach is only qualitative because the escape velocity is really only relevant if gravity is the only force acting on the dust grains. In the current problem, we expect two other strong forces to be in play: gas drag and radiation pressure. These could change the picture dramatically.

Obviously, μm -sized particles in the coma evolve much faster under the effect of gas drag and radiation pressure. Using the resolved coma images obtained with the Pic du Midi 1-m reflector (kindly provided by F. Colas on February 4 and 5), and those obtained from IAC-80 and other instruments (Table 3), we have found an ejection velocity of $250 \pm 80 \text{ m s}^{-1}$, which is smaller than the value given by Colas & Maquet in CBET2160 (Trigo-Rodríguez et al. 2010). This result suggests that the outburst probably occurred around February 2.30.

Information about dust production for the different particle sizes can be obtained. In order to discuss the rate of activity of comets, we usually measure the rate of activity of the nucleus $Af\rho$, typically

Table 3. Selected measurements of the coma diameter of SW1 during the massive outburst experienced on 2010 February 2. For more details, see the text.

Date (JD)	Observatory	Apparent coma diameter (arcsec)	Coma diameter ($\times 10^3$ km)
245 5230.68	442	19.2	73 ± 7
245 5231.43	458	23.5	86 ± 9
245 5232.43	458	30.6	93 ± 9
245 5232.48	IAC-80	27.4	103 ± 10
245 5233.49	442	30.4	114 ± 7
245 5233.58	IAC-80	32.2	121 ± 12
245 5234.47	458	42.3	160 ± 15
245 5238.69	442	49.6	186 ± 16

given in cm. This parameter (defined by A’Hearn et al. 1984) is a measure of the dust production rate, which does not attempt to disentangle the effects of albedo A , filling factor f and aperture ρ . Thus, it allows direct comparison between data sets obtained with different instruments. This parameter can be computed from the following equation given by A’Hearn et al. (1984):

$$Af\rho = \left[\frac{(2\Delta r)^2}{\rho} \right] \frac{F_{\text{com}}}{F_{\odot}}. \quad (2)$$

Here, Δ and r are the geocentric and heliocentric distances in au, ρ is the diameter of the photometric aperture in km, and F_{com} and F_{\odot} are the cometary and solar fluxes in the respective filters. The measured $Af\rho$ values for the R and I filters are shown in Fig. 6. In a similar way in which we noted how the I magnitude increases during an outburst, it is clearly visible in Fig. 6 that the production of large grains after the 2010 February 3 outburst is announced by a significant increase in the $Af\rho$ value in the I band. Returning to quiet activity, the $Af\rho$ values in the R and I bands tend to become similar, as in the data before the outburst. Consequently, it seems that such behaviour in the I band could be used to predict outbursts in the future.

Recently, the unexpected second massive outburst of comet 17P/Holmes has provided interesting clues on the nature of these outbursts. For example, it was previously proposed that the scale of the 17P outburst could be explained by the disintegration of one of the outer layers, which after the separation from the surface would have broken apart into the μm -sized dust observed in the coma (Sekanina 2007; Thomas, Alexander & Keller 2008). Dello Russo et al. (2008) found that the spatial distributions of measured volatiles in the coma are consistent with each other, and identified only a minor contribution from sublimating icy grains in their observing aperture. We interpret these observations as for most volatiles being produced by the explosive sublimation of the ice-rich surface on a very constrained time-scale. The largest particles became fine dust during the first stages of expansion, and only a few particles contributed to enhance the amount of volatiles in the coma as a result of additional sublimation in the later days.

4.3 Evolution of 29P outbursts

The massive release of particles triggering the outbursts seems to be produced typically from active areas on the surface. Two plausible scenarios are that (i) the volatile-rich areas are activated when the Sun rises on the local horizon or (ii) the outbursts are produced by a subsurface process that takes place at any local hour (as a result of heat conduction effects). Whatever the process is, a massive release of particles is produced during the outburst. Large and fresh

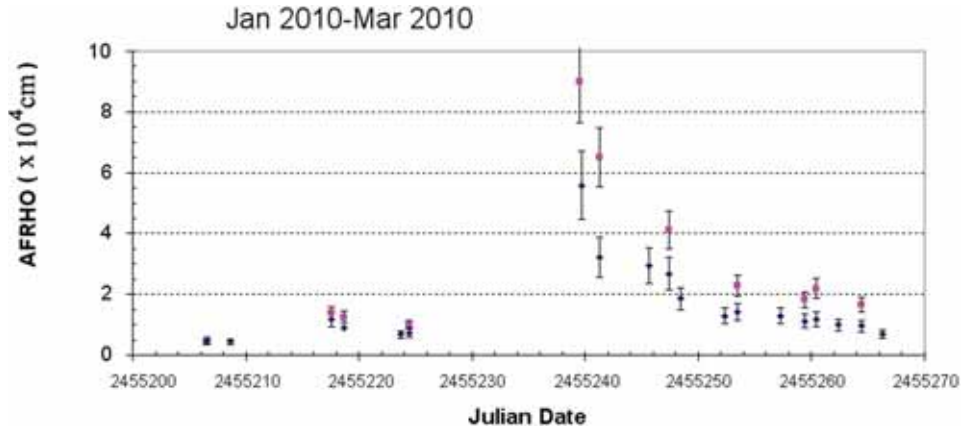


Figure 6. Computed $Af\rho$ values for the main outburst detected in 2010 January–March period. Blue dots are computed from R photometric band data and pink squares for the I band.

particles reaching the coma are efficiently heated by the Sun, so their sublimation starts. Then, the progressive fragmentation of these particles takes place in a second stage of the outburst, increasing the number density of μm -sized dust, and consequently increasing the brightness in R and V . The particles are released, forming a fan, but later the coma becomes pseudo-spherical (globule-like) as the fine dust expands outwards (see, for example, Figs 3 and 4). By doing so, the surface brightness of the coma decreases, as expected, as a consequence of the decrease in the number spatial density of dust in the line of sight. An outburst is announced by a sudden increase in the comet magnitude, produced by a massive injection of particles to the coma from an active region. Ulterior sublimation of the ice-rich dust produces a progressive increase in the spatial density of μm -sized dust, which starts to reflect light to produce the outburst in the optical range.

However, our results indicate that the 29P outbursts are periodic, and so are necessarily produced by nuclear activity. Consequently, it is not necessary to invoke the impact of meteoroid-sized bodies against the cometary nucleus to explain these (Gronkowski 2004). Of course, in statistically limited cases, this type of event would be behind the excavation of the surfaces of dormant comets, acting as a triggering mechanism. In any case, the fascinating behaviour of comet 29P suggests that it is a pristine object, which would be a good target for exploration by future space missions.

5 CONCLUSIONS

We have presented an unprecedented effort to monitor the photometric behaviour of comet 29P using different Johnson–Kron–Cousin filters. As a byproduct of this monitoring, we have been able to infer information about the development and nature of these processes. We summarize our findings as follows.

(i) We have demonstrated that multiband monitoring of the activity of 29P can be used to study the physical processes behind the development of cometary outbursts. Future high-resolution spectroscopic observations before, during and after the outbursts are encouraged. In particular, such observations would help us to better understand the processes involved in the sublimation and fragmentation of the particles, which we propose here.

(ii) Finally, we think that we have been able to constrain the rotation period of the nucleus of 29P from photometric data. PDM periodograms show a 50-d periodicity, which we consider a tentative

value for the rotation period of this centaur that fits most of the outbursts recorded from 2002 to 2010. Such a periodicity is also corroborated by the photometric profile produced by the presence of two active regions on the surface of 29P in the period 2008 December to 2009 February.

(iii) The average outburst frequency during the full monitored period is 49 d. Note that this value is consistent with the deduced rotation period in (ii). Such a frequency corresponds to 7.4 outbursts per yr, which is very close to the value previously found by our team (Trigo-Rodríguez et al. 2008). In consequence, the outburst activity of 29P is periodic, so the triggering mechanism for outbursts is the periodic insolation of an active region.

(iv) The brightest outburst observed during the last few years took place on 2010 February 2.3. The maximum computed values ($56\,000\text{ cm}$) in the R band exemplify well the energy driven by these outbursts. A follow-up of the particles using resolved images of the expanding coma indicate that the particles were ejected with a velocity of $250 \pm 80\text{ m s}^{-1}$.

ACKNOWLEDGMENTS

We are grateful for the valuable comments and encouragement received from Dr A. Fitzsimmons (Queen’s University, Belfast). We also appreciate a detailed and very constructive review received from Dr Jacques Crovisier. We thank the Grup d’Estudis Astronòmics (GEA) for providing the reduction software used in the present studies, in particular the LAIA and AVE programs developed by R. Barberà and J. A. Cano. Part of this work is based on observations made with the IAC-80 telescope under the Spanish Instituto de Astrofísica de Canarias Comisión de Asignación de Tiempo (CAT) service time. The IAC-80 is operated by the Instituto de Astrofísica de Canarias at the Observatorio del Teide. DAGH acknowledges support for this work from the Spanish MICINN under the 2008 Juan de La Cierva programme and under grant AYA-2007-64748.

REFERENCES

- A’Hearn M., Schleicher D. G., Millis R. L., Feldman P. D., Thompson D. T., 1984, *AJ*, 89, 579
- Belton M. J. S. et al., 2007, *Icarus*, 187, 573
- Belton M. J. S., Feldman P. D., A’Hearn M. F., Carcich B., 2008, *Icarus*, 198, 189

- Cabot H., Enzian A., Klinger J., Majolet S., 1997, in Greenberg J. M., ed., Proc. NATO Adv. Study Inst., NATO ASI Ser. C, Vol. 487, The Cosmic Dust Connection. Reidel, Dordrecht, p. 487
- Deeming T. J., 1975, *Ap&SS*, 36, 137
- Dello Russo N., Vervack R. J., Jr, Weaver H. A., Montgomery M. M., Deshpande R., Fernández Y. R., Martin E. L., 2008, *ApJ*, 680, 793
- Escolà-Sirisi E., Juan-Samsó J., Vidal-Sáinz J., Lampens P., García-Melendo E., Gómez-Forrellad J. M., Wils P., 2005, *A&A*, 434, 1063
- García-Melendo E., Clement C. M., 1997, *AJ*, 114, 1190
- Gronkowski P., 2004, *Astron. Nach.*, 325, 343
- Jewitt D., 1990, in Lagerkvist C. I., Rickman H., Lindblad B. A., eds, Proc. Asteroids, Comets, Meteors III. Astronomiska Observatoriet, Uppsala, Sweden, p. 347
- Jewitt D., 2008, in Altwegg K., Benz W., Thomas N., eds, *Trans-Neptunian Objects and Comets*. Springer, Berlin, p. 1
- Landolt A., 1992, *AJ*, 104, 340
- Marsden B., Williams G. V., 2003, *Catalogue of Cometary Orbits*, XVth edn. Smithsonian Astrophysical Observatory, Cambridge MA
- Meech K., Belton M., Mueller B., Dicksion M., Heide R., 1993, *AJ*, 106, 1222
- Moreno F., 2009, *ApJS*, 183, 33
- Prialnik D., 2000, *Earth, Moon, Planets*, 89, 27
- Samarasinha N. H., Mueller B. E. A., Belton M. J. S., Jorda L., 2004, in Festou M. C., Keller H. U., Weaver H. A., eds, *Comets II*. Univ. Arizona Press, Tucson, p. 281
- Sekanina Z., 1982, in Wilkening L. L., ed., *Comets*. Univ. Arizona Press, Tucson, p. 251
- Sekanina Z., 2007, *Central Bureau Electron. Tel.*, 1118
- Sheppard S. S., Lacerda P., Ortiz J. L., 2008, in Barucci M. A., Boehnhardt H., Cruikshank D. P., Morbidelli A., eds, *The Solar System Beyond Neptune*. Univ. Arizona Press, Tucson, p. 129
- Snodgrass C., Lowry S. C., Fitzsimmons A., 2006, *MNRAS*, 373, 1590
- Stansberry J. A. et al., 2004, *ApJS*, 154, 463
- Stellingwerf R. F., 1978, *ApJ*, 224, 953
- Stetson P. B., 2000, *PASP*, 112, 925
- Thomas N., Alexander C., Keller H. U., 2008, *Space Sci. Rev.*, 138, 165
- Trigo-Rodríguez J. M., Blum J., 2009, *Planet. Space Sci.*, 57, 243
- Trigo-Rodríguez J. M., García-Melendo E., Davidsson B. J. R., Sánchez A., Rodríguez D., Lacruz J., De los Reyes J. A., Pastor S., 2008, *A&A*, 485, 599
- Trigo-Rodríguez J. M., Sanchez A., Colas F., Maquet L., Pastor S., Reyes J. A., Rodríguez D., Kugel F., 2010, *Central Bureau Electron. Tel.*, 2160
- Whipple F. L., 1980, *AJ*, 85, 305

This paper has been typeset from a $\text{\TeX}/\text{\LaTeX}$ file prepared by the author.